



Fabrication and Characterization of CuO Nanofibers using Nanofiber Generator

R.G. Sethuraman¹, T. Venkatachalam^{2*}, E.P. Subramaniam³, T.V. Viknesh⁴, V. Manikandan⁴

¹Department of Physics, Kumaraguru College of Technology, Coimbatore, TN, India

²Department of Physics, Coimbatore Institute of Technology, Coimbatore, TN, India

³Department of Chemistry, Coimbatore Institute of Technology, Coimbatore, TN, India

⁴Department of Electrical & Electronics Engineering, Coimbatore Institute of Technology, Coimbatore, TN, India

Received: 22.02.2018 Accepted: 27.03.2018 Published: 30-06-2018

*tvenkatachalam@cit.edu.in

ABSTRACT

An improvised electro-spin coating unit was designed, fabricated and optimized to fabricate Nano-fibers. Composite nanofibers of CuO (dissolved in PVA) were fabricated using this unit. The prepared fibers were annealed at three different temperatures (400 °C, 500 °C and 600 °C) using a muffle furnace, and all the continuous fibers were broken down to nanocrystals. The structural and composition of the nanocrystals were analyzed using XRD and EDAX measurements. The X-ray diffraction peaks revealed that the crystals are monoclinic crystalline structure. The composition of the crystal is confirmed as CuO from the percentage of constituents of Copper and Oxygen in EDAX results. The optical properties of the fibers were studied by using a spectrophotometer. The optical band gap energy is found to be nearly 2 eV. The surface morphology of the crystal was studied using FESEM analysis. The crystals are found to be defect-free, and they are excellent material for high sensitive optoelectronic sensors.

Keywords: Bandgap; CuO; EDAX; FESEM; Monoclinic crystal; Nanocrystals; Nanofiber; Nanofiber generator; Optoelectronic sensors; XRD.

1. INTRODUCTION

In recent years, nanostructured metal oxide materials have been proven as a milestone in modern electronic products. They exhibit excellent electronic, optical, mechanical properties and many more for all intelligent systems, including embedded systems. Among metal oxides, transition metal oxides, specifically Copper (II) Oxide (CuO) is a well-known semiconductor (P-type) with a bandgap of 2.0 eV. It also has a wide range of applications such as optoelectronic sensors (Mathews *et al.* 2010), gas sensors (Zhang *et al.* 2009; Duc *et al.* 2014), high-Tc superconductors, magnetic storage devices, Environmental sensors, catalyst (Jun *et al.* 2009), antioxidant photoelectrical, photothermal, antibacterial (Torres *et al.* 2010), etc. Various methods, such as thermal methods, chemical methods, electrochemical method, hydrothermal method, decomposition method, etc., were adopted for the fabrication of nanocrystals. In this research, electrospinning technique (Kim *et al.* 2008; Thangavel *et al.* 2016) is being used to prepare nanofibers of CuO-PVA and subsequent annealing to remove PVA and then to fabricate nanocrystals of CuO. This novel method of synthesis is an efficient and simple method of preparing nanoparticles with high yield at low cost.

2. EXPERIMENTAL DETAILS

2.1 Preparation of Precursor Solution

The precursor solution of CuO was prepared using the following procedure. 5g of Copper Acetate (Merk grade) and 3 g of NaOH (Merk grade) were weighed using a single pan balance (accuracy 0.001 mg) and transferred to agar mortar and grounded one after another for 5min. The obtained fine powders were mixed with 6 ml of PEG 400 (Polyethylene glycol 400) and grinded for 30 min using a mortar. The obtained paste was thoroughly washed with distilled water and then with ethyl alcohol twice to remove the PEG 400 in order to control the size of the nanoparticles. The paste was dried at 70 °C in an oven for 2 hours. The resultant solid granules were subsequently annealed at 400 °C, 500 °C and 600 °C in a muffle furnace for 2 hours and cooled to room temperature. The fine powders were mixed with PVA (analytical grade) and preserved separately in different vials. The complete experimental procedure in this research is depicted as a flow chart given below (Fig.1).

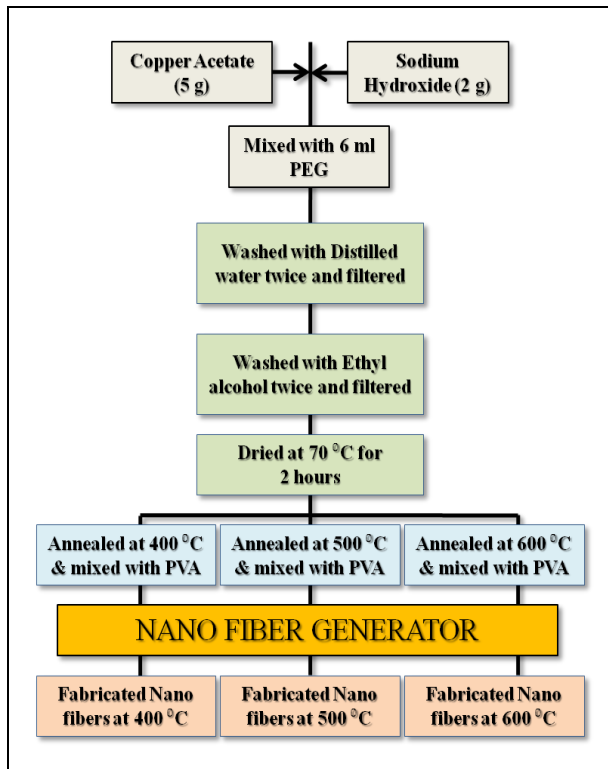


Fig. 1: Flow chart of the nanofiber synthesis.

2.2 Nanofiber Generator

The microcontroller-based electrospinning nanofiber generating unit was identified for the preparation of CuO nanofiber in this research. The unit was designed and fabricated using the electronic components in the laboratory, as shown in the schematic diagram Fig.2. It consists of three major units i) High voltage power supply (0 to 30 kV), ii) Nanofiber producing unit, and iii). Nanofiber collecting unit. The microcontroller (PIC 16F877A) fitted board was connected with the computer, and the operating voltage was drawn from the 6V DC power supply unit. Using test solution (appropriate viscous sugar solution) in the syringe, the flow of liquid from the tip of the stainless needle was assured. Another similar programmed microcontroller fitted board and the inverter (with potentiometer) are attached along with the line output transformer (LOT), and the output terminals were connected across the needle of the syringe, and the substrate fitted metal holder to apply high voltage. The expected variation of voltage across the needle and the holder from 1 kV to 30 kV with adjustment of the potentiometer was measured, and the potentiometer was calibrated.

2.3 High Voltage Power Supply Unit

The variable high voltage power supply unit (microcontroller based) is used to generate 0-30 KV C voltage between the needle and the collecting unit. The

flyback transformer transforms energy and also stores energy for a small fraction of the switching period. It has a high reluctance of magnetic flux to store energy. In primary and secondary windings, the current does not flow simultaneously. The flyback transformer is a freely tied inductor rather than a classical transformer, in which current flow concurrently in all magnetically coupled windings. The primary winding of the flyback transformer is usually driven by a switch from a DC supply. The primary inductance induces the current to build up in a ramp when the switch is turned on. But when the switch is turned off, the current in the primary winding collapse. Then, as a result of this, the voltage in the output windings raises quickly. When the input current in the primary is switched off, an EMF is induced in the secondary and this time, diode conducts, as its polarities are different. This induced voltage is then rectified and filtered with a capacitor producing a DC output.

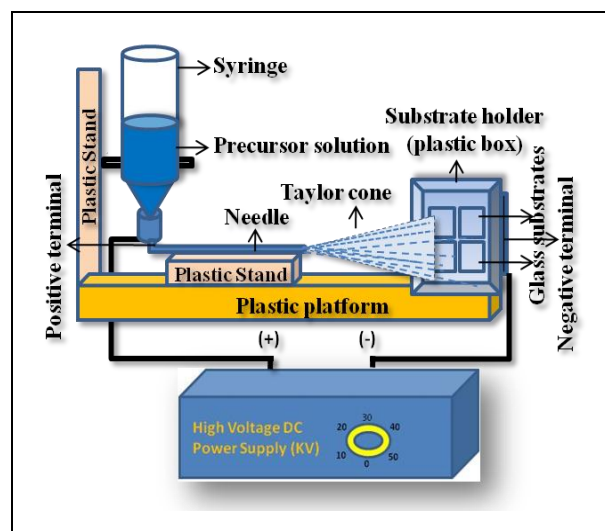


Fig. 2: Schematic diagram of nanofiber generator.

2.4 Nanofiber Producing Unit

The Spinneret solution feeding unit is made up of a syringe (with stainless steel needle of size (0.1mm to 0.3 mm)). The precursor solution is taken in the vertically mounted plastic syringe with the 'L' shaped metallic needle at the bottom so that the solution can ooze out as droplets in the tip of the needle by gravity. The diameter of the droplet is equal to the diameter of the needle (0.26 mm). The needle is fitted with positive, and the collecting unit is fitted to the negative of the power supply unit. The collecting unit is having a brass plate pasted on a vertical plastic stand, and a thin plastic box without a lid is fitted over it with four well-cleaned substrates of size 1cm x 1cm. The needle and the collecting unit are placed at the same level and 5cm to 8 cm apart. The whole arrangement is placed inside a plastic box so that the nanofiber could not pollute the outside system. Here the applied field is very large, so there is the penetration of

the electric field taking place. As soon as the droplet is formed at the tip of the needle, due to the electric field, a Taylor cone is formed, and fibers are deposited on the four glass plates. The plastic boxes with glass substrates were collected after deposition and covered with their lids, and labelled for further characterizations.

2.5 Nanofiber Collecting Unit

Many methods are adopted to collect the generated nanofiber. One of the popular methods is by using a flat plate collector, which generates nonaligned nanofiber. This is a cheaper method of producing nanofibers in the glass plate, which is connected to a high voltage negative potential. During nanofiber generation, the collector must be grounded or maintained at high negative potential. When a high voltage is applied, the electrostatic force is exerted across the spinneret and the collector. The collector draws the polymer solution from the spinneret in the form of the nanofiber, and the generated nanofiber is deposited on the surface of the collector.

2.6 Preparation of CuO Nanofibers

The high voltage power supply is mandatory in electro-spinning technology to spawn the nanofibers. Syringe pump, also known as spinnerets, are small pumps precisely operated by their own gravity action. When the prepared nanopowders are dissolved in ethyl alcohol and kept in a sonicator for 15 min to get a homogeneous solution and then it is filled in the syringe (fiber producing unit). With the help of high voltage, an applied electric field is applied in between the spinneret and collector. The collector draws the polymer solution from the spinneret in the form of nanofibers, and the generated nanofibers are then coated on the surface of the collector. Thus the CuO nanofibers are fabricated from the microcontroller-based electro-spinning method.

3. RESULTS AND DISCUSSION

3.1 X-ray Diffraction Analysis

Fig.3 shows the X-ray diffraction (XRD) pattern of the CuO nano fiber synthesized from copper acetate and sodium hydroxide by solid-state synthesis method. The XRD diffraction studies were carried out for the samples annealed at 400 °C, 500 °C and 600 °C separately. The XRD pattern revealed the orientation and crystalline nature of copper oxide nanofiber. The peak position with 2θ value of 32.50 °, 38.80 ° and 48.81 ° are indexed as (110), (200), ($\bar{2}$ 02) planes, which are in good agreement with those of powder CuO obtained from the International Center of Diffraction Data card (JCPDS-895895) conforming the formation of crystalline monoclinic structure. The lattice parameters are $a=4.639$

\AA , $b = 3.468 \text{\AA}$ and $c = 6.241 \text{\AA}$ and $\alpha = \gamma = 90^\circ$, $\beta = 99.5^\circ$.

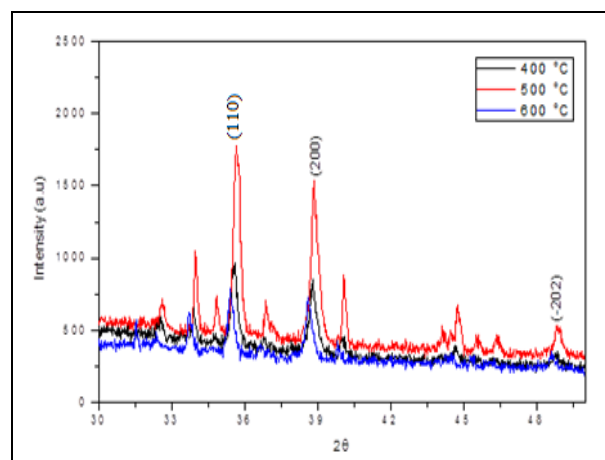


Fig. 3: XRD pattern of the nanocrystals.

The obtained results are well consistent with the previously reported literature (Langford *et al.* 1991; Abaker *et al.* 2011). The crystalline size (D) is calculated using Scherrer's formula ($D = \frac{0.94 \lambda}{\beta \cos \theta}$). The full width at the half maximum (β) is calculated for the slope of $\beta \cos \theta$ versus $\sin \theta$ plot using the relation $\beta = \frac{\lambda}{D \cos \theta} - \epsilon \tan \theta$. The dislocation density (δ) is calculated from the relation $\delta = 1/D^2$. The lattice parameters (a , b & c) of the crystals were determined by using the relation.

$$\frac{1}{d^2} = \frac{h^2}{a^2 \sin^2 \gamma} + \frac{k^2}{b^2 \sin^2 \gamma} - \frac{2hk \cos \gamma}{ab \sin^2 \gamma} + \frac{l^2}{c^2}$$

Where (hkl) is the Miller indices of the predominant peaks.

3.2 Optical Analysis

UV-Vis-NIR spectroscopy study was carried out on the samples of CuO nanofibres annealed at different temperatures such as 400°C, 500°C and 600 °C. The observed absorbance spectrum shows that the minimum cut-off wavelength of 300 nm, 314 nm and 317 nm, respectively. The role of annealing temperature has a considerable effect on the grain size of the particle, whereas the crystalline nature increases with respect to an increase in its annealing effect. It induces a strain mediated effect on the sample of CuO, which improves the role of layers leads to the increase in the absorption edge of the sample. The surface trapping effect of grain boundaries minimizes its effective strength with respect to the annealing. Hence there is an increase in its absorption edge. The increasing redshift with decreasing particle size suggests that the defects responsible for the intra-gap states are primarily surface defects (Sukhorukov *et al.* 2006; Ovchinnikov *et al.* 2007;

Rehman *et al.* 2011) and show higher bandgap (Rehman *et al.* 2011; Koffyberg *et al.* 1982). The blue shift in the direct band edges, as seen in our case, is due to the quantum confinement effect (Rehman *et al.* 2011; Neeleshwar *et al.* 2005).

The absorption coefficient (α) is estimated from the Optical transmittance spectra using the relation $\alpha = 2.303 \log(100T) / t$ where T is the Transmittance (in %), and t is the thickness of the film. All the graphs satisfied the condition for direct transition in the excitation process (ie) $\alpha = (E_v - E_i)^{1/2}$ for allowed direct transition., where E_v is the top of the valence band and E_i the initial state from which the transition is made. The bandgap of the nanocrystals prepared at three temperatures 400 °C, 500 °C and 600 °C, were determined by extrapolating the curve in the graph drawn between $(\alpha h\nu)^2$ and $(h\nu)$. It is found that they are direct bandgap semiconductors having 1.95 eV, 2.09 eV and 2.28 eV, respectively and their bandgap increases with temperature.

3.3 FESEM and EDAX Analysis

The surface morphology and microstructure of pure CuO nanoparticles were investigated by using a Field emission scanning electron microscope (FESEM). As seen in the FESEM images (Fig.4), the crystallites are spherical at low temperature (400 °C) and are very fine rod-like at higher temperatures (500 °C), then it becomes nanocrystalline at 600 °C. It is also evident that the particle size decreases with an increase in annealing

temperature, which is consistent with XRD results calculated by Scherrer's equation. The presence of copper and oxide is confirmed in the EDAX spectra (Fig.5), and its molecular formula is CuO.

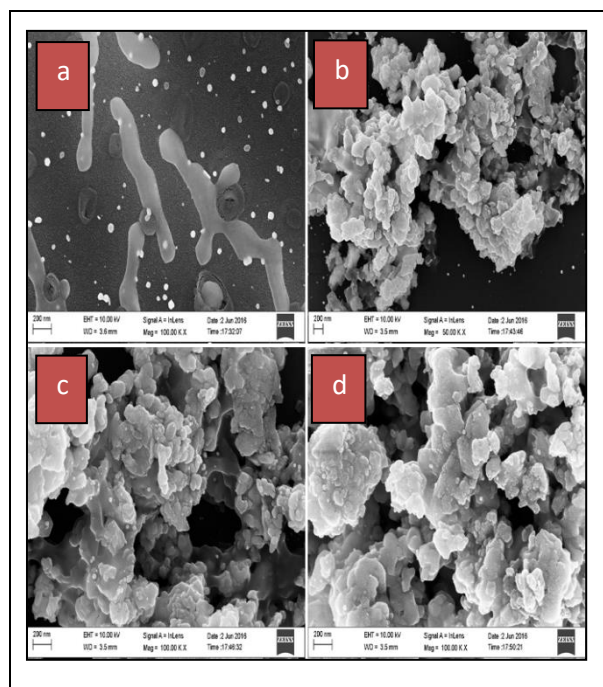


Fig. 4: FESEM images of the nanofibers annealed at a) 400 °C b) 500 °C c) 600 °C.

Table 1. Lattice parameter, crystalline size, stress, strain and dislocation density of nanocrystals.

Peak number	Temperature (°C)	(hkl)	2 θ (°)	Lattice parameter (Å)	Crystalline Size D (nm)	Stress (Mega Pascal)	Strain 10 ⁻⁴	Dislocation Density 10 ¹⁴ (m ⁻²)
1	400	110	35.508	a = 4.636	29.31	185.250	12.350	11.644
2		200	38.806	b = 3.418	22.74	238.785	15.919	19.338
3		$\bar{2}02$	48.819	c = 6.262	23.68	229.365	15.291	17.838
Average values					25.24	217.800	14.520	16.273
1	500	110	35.509	a = 4.628	25.49	212.955	14.198	15.379
2		200	38.878	b = 3.421	22.87	237.495	15.833	19.126
3		$\bar{2}02$	48.901	c = 6.253	26.66	203.655	13.578	14.065
Average values					25.00	218.035	14.54	16.190
1	600	110	31.562	a = 4.654	26.87	205.320	13.688	13.845
2		200	38.645	b = 3.566	22.04	246.311	16.412	22.048
3		$\bar{2}02$	48.852	c = 6.209	23.85	227.564	15.171	17.978
Average values					24.25	226.390	15.09	17.950

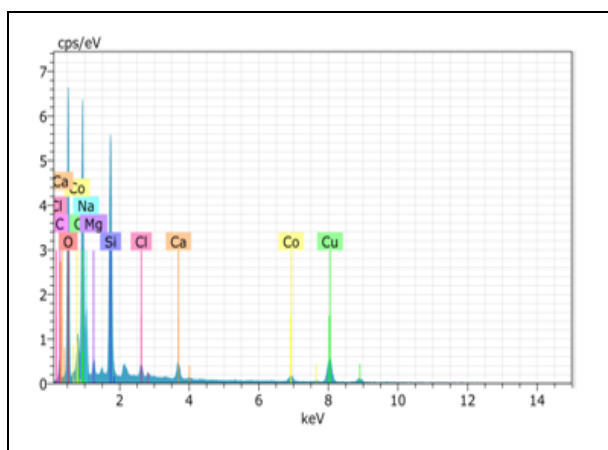


Fig. 5: EDAX Spectra of fabricated CuO nanofibers after annealing.

4. CONCLUSION

The nanocrystals of CuO with a monoclinic structure have been synthesized through a simple, low-cost solid-state reaction method. It has been noticed that improved crystallinity was observed when annealed at higher temperatures. The intensity of peaks has been increased with an increase in annealing temperature. The optical studies show CuO is the direct bandgap semiconductor, and the bandgap decreases with an increase in temperature. The FESEM results confirm the formation of nanocrystals precisely at higher annealing temperatures. Also, the EDAX results confirm the existences of CuO nanoparticles.

ACKNOWLEDGEMENTS

The authors would like to express their sincere thanks to Dr. S. R. K. Prasad (Correspondent, CIT), Dr. R. Prabhakar (Secretary, CIT), Dr. V. Selladurai (Principal, CIT), Mr. S. Rajiv Rangasamy (Director, CIT), Correspondent of KCT, Secretary of KCT and Principal of KCT for their help and encouragement during work.

FUNDING

This research received no specific grant from any funding agency in the public, commercial, or not-for-profit sectors.

CONFLICTS OF INTEREST

The authors declare that there is no conflict of interest.

COPYRIGHT

This article is an open access article distributed under the terms and conditions of the Creative Commons Attribution (CC-BY) license (<http://creativecommons.org/licenses/by/4.0/>).



REFERENCES

- Abaker, M., Umar, A., Baskoutas, S., Kim S. H. and Hwang, S. W., Structural and optical properties of CuO layered hexagonal discs synthesized by a low-temperature hydro-thermal process, *J. Phys. D: Appl. Phys.*, 44, 155405(2011).
<https://doi.org/10.1088/0022-3727/44/15/155405>
- Duc, L. D., Le, D. T. T., Van Duy, N., Hoa, N. D. and Van Hieu, N., Single crystal cupric oxide nanowires: Length- and density-controlled growth and gas-sensing characteristics, *Physica E: Low-dimensional Systems and Nanostructures*, 58, 16-23(2014).
<https://doi.org/10.1016/j.physe.2013.11.013>
- Jun, J., Jin, C., Kim, H., Park, S. and Lee, C., Fabrication and characterization of CuO-core/TiO₂-shell one-dimensional nanostructures, *Appl. Surf. Sci.*, 255, 8544-8550(2009).
<https://doi.org/10.1016/j.apsusc.2009.06.006>
- Kim, Y-S., Hwang, I-S., Kim, S-J, Lee, C-Y. and Lee, J-H., CuO nanowire gas sensors for air quality control in automotive cabin, *Sensors and Actuators B: Chemical*, 135, 298-303(2008).
<https://doi.org/10.1016/j.snb.2008.08.026>
- Koffyberg F. P. and Benko, F. A., A photoelectrochemical determination of the position of the conduction and valence band edges of p-type CuO, *J. Appl. Phys.*, 53, 1173-1177(1982).
<https://doi.org/10.1063/1.330567>
- Langford J. I. and Louer, D., High-resolution powder diffraction studies of copper(II) oxide, *J. Appl. Crystallogr.*, 24, 149-155(1991).
<https://doi.org/10.1107/S0021889890012092>
- Mathews, N., Varghese, B., Sun, C., Thavasi, V., Andreasson, B. P., Sow, C. H., Ramakrishna, S. and Mhaisalkar, S. G., Oxide nanowire networks and their electronic and optoelectronic characteristics, *Nanoscale*, 2, 1984–1998(2010).
<https://doi.org/10.1039/c0nr00285b>

- Neeleshwar, S., Chen, C. L., Tsai, C. B., Chen, Y. Y., Chen, C. C., Shyu S. G. and Seehra, M. S., Size-dependent properties of CdSe quantum dots, *Phys. Rev. B.*, 71, 201307(R) (2005).
<https://doi.org/10.1103/PhysRevB.71.201307>
- Ovchinnikov, S. G., Gizhevskii, B. A., Sukhorukov, Y. P., Ermakov, A. E., Uimin, M. A., Kozlov, E. A., Kotov Y. and Bagazeev, A.A.V., Specific features of the electronic structure and optical spectra of nanoparticles with strong electron correlations, *Phys. Solid State*, 49, 1116-1120(2007).
<https://doi.org/10.1134/S1063783407060169>
- Rehman, S., Mumtaz, A. and Hasanain, S. K., Size effects on the magnetic and optical properties of CuO nanoparticles, *J. Nanopart. Res.*, 13, 2497-2507(2011).
<https://doi.org/10.1007/s11051-010-0143-8>
- Sukhorukov, Y. P., Gizhevskii, B. A., Mostovshchikova, E. V., Yermakov, A. Y., Tugushev S. N. and Kozlov, E. A., Nano-crystalline copper oxide for selective solar energy absorbers, *Tech. Phys. Lett.*, 32, 132-135(2006).
<https://doi.org/10.1134/S1063785006020131>
- Thangavel, K., Kannuamy, R., Balamurugan A. and Mahendran, R., Design and construction of micro-controller based electrospinningnanofiber generator, *Advanced Science Letters*, 22,1076-1079(2016).
<https://doi.org/10.1166/asl.2016.6968>
- Torres, A.,Ruales, C.,Pulgarin, C.,Aimable, A., Bowen, P.,Sarria,V. and Kiwi, J., Innovative High-Surface-Area CuOPretreated Cotton Effective in Bacterial Inactivation under Visible Light, *ACS Appl. Mater. Interfaces*,2(9), 2547-2552(2010).
<https://doi.org/10.1021/am100370y>
- Zhang, Z., Li, X., Wang, C., Wei, L., Liu, Y. and Shao, C., ZnO Hollow nanofibers: Fabrication from facile single capillary electrospinning and applications in gas sensors, *J. Phys. Chem. C*, 113, 19397-19403(2009).
<https://doi.org/10.1021/jp9070373>